

## **Werk**

**Jahr:** 1970

**Kollektion:** fid.geo

**Signatur:** 8 Z NAT 2148:36

**Werk Id:** PPN101433392X\_0036

**PURL:** [http://resolver.sub.uni-goettingen.de/purl?PID=PPN101433392X\\_0036](http://resolver.sub.uni-goettingen.de/purl?PID=PPN101433392X_0036) | LOG\_0015

## **Terms and Conditions**

The Goettingen State and University Library provides access to digitized documents strictly for noncommercial educational, research and private purposes and makes no warranty with regard to their use for other purposes. Some of our collections are protected by copyright. Publication and/or broadcast in any form (including electronic) requires prior written permission from the Goettingen State- and University Library.

Each copy of any part of this document must contain there Terms and Conditions. With the usage of the library's online system to access or download a digitized document you accept the Terms and Conditions.

Reproductions of material on the web site may not be made for or donated to other repositories, nor may be further reproduced without written permission from the Goettingen State- and University Library.

For reproduction requests and permissions, please contact us. If citing materials, please give proper attribution of the source.

## **Contact**

Niedersächsische Staats- und Universitätsbibliothek Göttingen  
Georg-August-Universität Göttingen  
Platz der Göttinger Sieben 1  
37073 Göttingen  
Germany  
Email: [gdz@sub.uni-goettingen.de](mailto:gdz@sub.uni-goettingen.de)

## **Time Variation of Low Energy Protons in the Inner Radiation Belt**

By E. ACHTERMANN, S. C. FREDEN<sup>2)</sup> and D. HOVESTADT<sup>1)</sup>

Eingegangen 21. Januar 1969

*Summary:* By means of a French RUBIS-rocket, launched in April 1966 from Hamaguir (Algerian Sahara), measurements of protons in the inner radiation belt have been performed.

With two solid state detector range telescopes and two solid state detector omnidirectional counters the proton energy ranges 1.3 to 13 MeV, 5.2 to 44 MeV, 2.7 to 4.5 MeV, 4.5 to 8.0 MeV, 8.0 to 12 MeV, 12 to 25 MeV (telescopes) and 6 to 20 MeV and 40 to 80 MeV (omnidirectional counters) have been covered. Differential energy spectra were obtained in the region of B, L-space from  $L = 1.46$ ;  $B = 0.223$  to  $L = 1.665$ ;  $B = 0.168$ . The flux of protons for B, L values with a minimum altitude above 700 km agrees within a factor of less than 2 with previous measurements. With decreasing minimum altitude the measurements show a significantly lower flux of low energy protons compared to previous data. Protons with energies above 20 MeV do not show a significant flux variation.

*Zusammenfassung:* Mit einer französischen RUBIS-Rakete wurden im April 1966 von Hamaguir (Algerische Sahara) Messungen von Protonen im inneren Strahlungsgürtel durchgeführt.

Mit zwei Halbleiterzählerteleskopen und zwei Omnidirektionalzählern wurden Protonenflüsse in den Energiebereichen 1,3 bis 80 MeV gemessen.

Differentielle Energiespektren wurden im Bereich des B, L-Raumes von  $L = 1,46$ ,  $B = 0,223$  bis  $L = 1,665$ ,  $B = 0,168$  erhalten.

Die Protonenflüsse in B, L-Bereichen mit Minimumshöhe oberhalb 700 km stimmen innerhalb eines Faktors 2 mit bisherigen Messungen überein. Mit abnehmender Minimumshöhe zeigen die Messungen einen signifikant erniedrigten Fluß von niederenergetischen Protonen im Vergleich zu älteren Messungen. Oberhalb 20 MeV tritt die Flußerniedrigung nicht auf.

### **Introduction**

In April 1966, a sounding rocket experiment for measuring trapped protons in the inner radiation belt was performed. The rocket, a French RUBIS, was launched from the French rocket launching site in the Algerian Sahara and reached a maximum altitude of 2035 km. In addition to the energetic particle experiment an electron density experiment and a barium vapor cloud experiment were included in the payload.

---

<sup>1)</sup> DR. EBERHARD ACHTERMANN, DR. STANLEY C. FREDEN und DR. DIETRICH HOVESTADT, Max-Planck-Institute for Physics and Astrophysics, Institute for Extraterrestrial Physics, Garching near Munich.

<sup>2)</sup> Permanent Address: NASA Manned Spacecraft Center, Houston, Texas.

The energetic particle experiment was performed by four devices: two proton range telescopes and two omnidirectional detectors similar to the detectors already flown by FREDEN et al. [1965]. The trajectory of the rocket covered the range of B, L-space between  $L = 1.665$ ,  $B = 0.168$  gauss and  $L = 1.44$ ,  $B = 0.226$  gauss. During the flight the rocket had a spin rate of about 5.5 rps with a precession angle starting at about  $5^\circ$  and increasing to about  $10^\circ$  at the end of the flight, as measured with an on-board search coil magnetometer.

Experiment Setup

a. Telescopes

Each of the telescopes consisted of a stack of four surface barrier silicon detectors and absorbers, wich was heavily shielded on the sides and on the back. The opening half angle of about  $17^\circ$  was defined mainly by the first two detectors of each device. Figure 1 shows a cross-sectional view of one of the telescopes. The energy ranges of the output channels were defined by the ranges of the protons within each sandwich. A coincidence-anticoincidence-logic decided in which detector or absorber of the stack the protons stopped. In addition to the coincidence outputs the singles counting rates of the first detectors were counted in the digital channels IA and IIA and with high speed rate-meters. The time constants of the rate-meters were about 1/20 second which is short compared to the rotation period of the rocket. A broom magnet in the aperture bends electrons up to an energy of 600 KeV so that they are hindered to enter the detector stack. Table 1 shows the telescopes' characteristics.

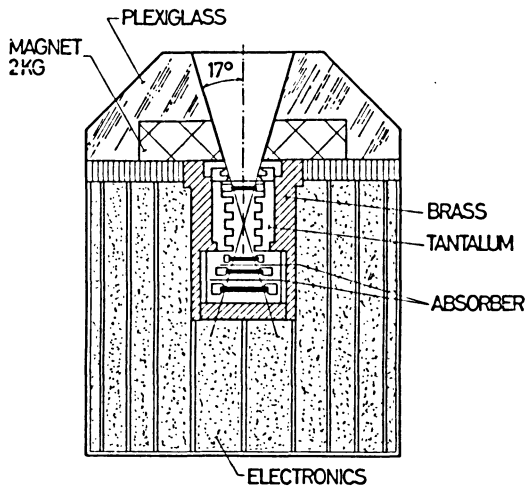


Figure 1: Cross-sectional view of telescope II.

Table 1: Detector Telescope Characteristics.

Telescope I				Telescope II			
Output Channel	Geometric Factor (cm <sup>2</sup> ster)	Energy Range (MeV)		Output Channel	Geometric Factor (cm <sup>2</sup> ster)	Energy Range (MeV)	
IA	0.074	1.3—13		IIA	0.20	5.2—44	
IAB $\bar{C}$	0.015	2.7— 4.5		IIAB $\bar{C}$	0.029	8.0—12.0	
IABCD $\bar{D}$	0.015	4.5— 8.0		IIABCD $\bar{D}$	0.029	12.0—25	

Detector	Area	Thickness	Bias (MeV)	Detector	Area	Thickness	Bias (MeV)
A	.20 cm <sup>2</sup>	53 micron	.330	A	.455 cm <sup>2</sup>	270 micron	.700
B	.20 cm <sup>2</sup>	109 micron	.400	B	.450 cm <sup>2</sup>	281 micron	.700
C	.40 cm <sup>2</sup>	100 micron	.400	C	.950 cm <sup>2</sup>	306 micron	.700
D	.85 cm <sup>2</sup>	300 micron	.600	D	1.95 cm <sup>2</sup>	300 micron	.700

The proton energy thresholds were measured with Van de Graaff proton accelerators in the energy range from 2.5 to 12.5 MeV. The measured energy thresholds were in good agreement with the calculated values from proton range-energy tables, which are shown in Figures 2a and 2b. Figure 2c shows the measured energy responses for both telescopes for the channels AB $\bar{C}$  and ABCD $\bar{D}$ . Both telescopes were fixed in the rocket at an angle of 45° with respect to its nominal spin axis. It can be shown [ACHTERMANN, 1967] that for this angle and for a magnetic field direction of 45° with respect to the spin axis, the mean counting rates of the telescopes would be proportional to the omnidirectional flux within about 11 percent. This condition was nearly fulfilled.

#### b. Omnidirectional counters

A cross-sectional view of the omnidirectional counters is shown in Fig. 3. Small cubical lithium drifted silicon detectors of the size 1 × 1 × 1 mm and 3 × 3 × 3 mm were mounted on the top of heavy shielding material. The higher energy detector (3 × 3 × 3 mm) was surrounded by a hemispherical brass-shield, giving the energy threshold of 40 MeV for protons. The lower energy detector was covered with 1 mg/cm<sup>2</sup> aluminized plastic foil. The solid angle of both devices was 2  $\pi$ . The upper energy limits of both detectors were determined by the energy deposition of the protons within the silicon cubes and by the electronic thresholds which were set at 0.3 MeV for electrons and 5.0 MeV for protons. These give the energy channels shown in Table 2 (see p. 32).

The geometric factors were calculated for particles with pitch angles of 90° (isotropy in a plane). The assumption of isotropy would not change the geometrical factors appreciably. Since the geometric factors are also somewhat dependent upon the

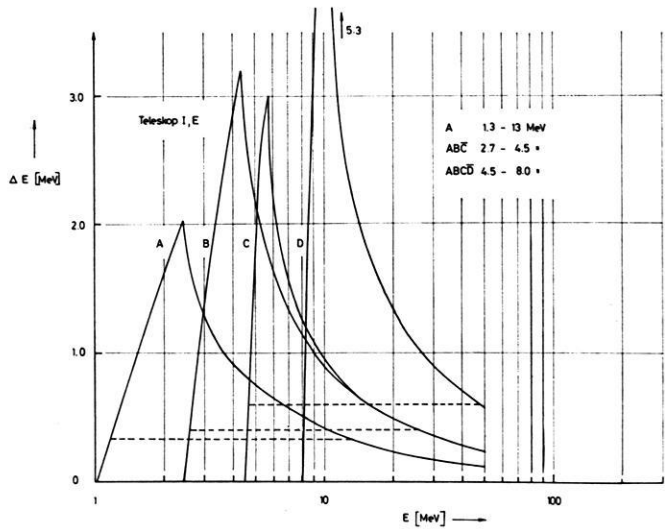


Figure 2a.

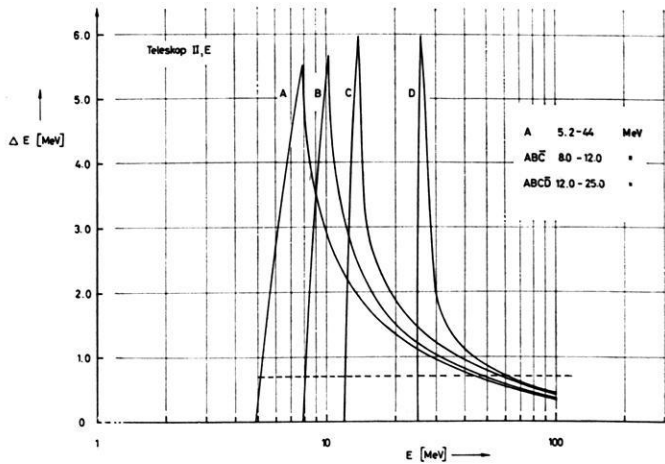


Figure 2b.

Figure 2a and 2b: The energy E, which is deposited in the different detectors of the two telescopes as a function of the energy of the incoming protons. The interrupted lines show the level of the discriminators.

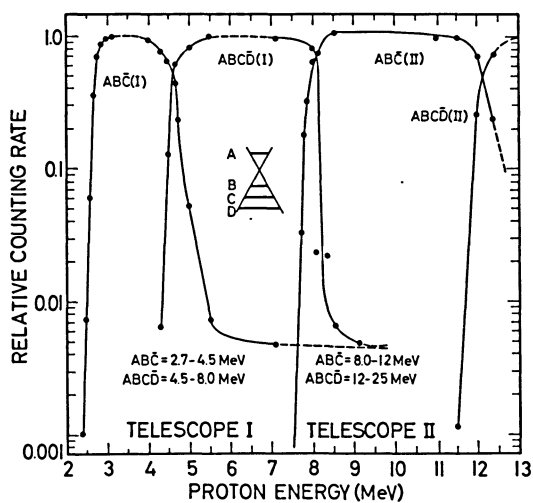


Figure 2c: Response measurement of the telescopes with proton accelerators.

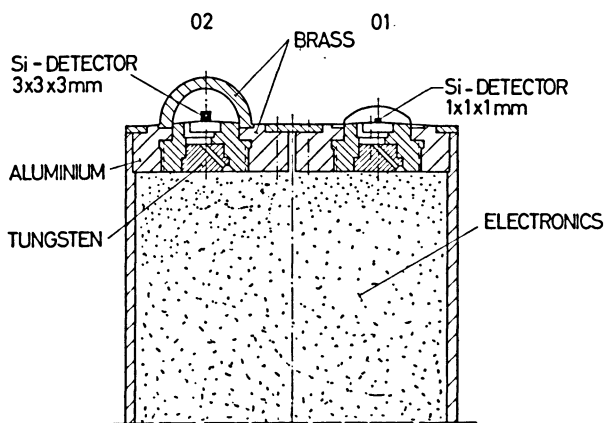


Figure 3: Cross-sectional view of the omnidirectional counters O9O (40–80 MeV) and OMO (6–20 MeV).

Table 2: Omnidirectional Detector Characteristics.

	Detector 1 (01)	Detector 2 (02)
Solid state detector size (mm)	$1 \times 1 \times 1$	$3 \times 3 \times 3$
Omnidirectional geometrical factor for protons in the 5 MeV bias channel ( $\text{cm}^2$ )	$(380 \pm 100)^{-1}$	$(21 \pm 3)^{-1}$
Detected particle energy ranges (MeV)		
5 MeV bias channel	p 6–20	p 40–80
0.3 MeV bias channel	p > 2	p > 40
	e > 0.3	e $\gtrsim$ 4.5

energy spectrum of the protons we used the slope of the spectrum as measured by the telescopes in the calculations.

The critical parameters in the calculation of the geometric factors are the sizes of the silicon cubes and the levels of the electronic thresholds. The uncertainties in the values of these measured parameters lead to uncertainties in the absolute flux values of  $\pm 20$  percent.

### Experimental Results

During the flight data were obtained from trapped particles at altitudes above 1000 km and L-values above  $L = 1.44$ . Figure 4 shows the number of counts per 5 seconds for most of the channels of the experiment as a function of time after launch. The arrows on the top of the figure indicate the B, L-locations where differential energy spectra are shown in the following Figs. 5 and 6. The 48 coefficient model of the earth magnetic field of JENSEN and CAIN [1962] is used for the B, L computation.

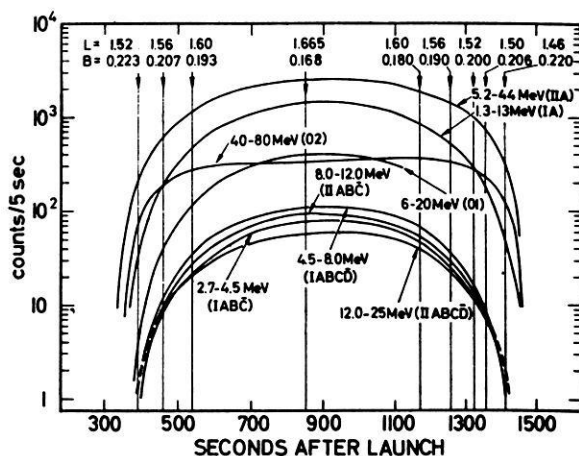


Figure 4: Mean counting rates/5 sec of all measured channels. The arrows indicate the positions in the B, L-space, where differential proton fluxes are drawn (see Figure 5 and 6).

The error bars indicate the statistical errors only. The spectrum at the higher B-value for each L-value corresponds to the upward moving rocket, the other spectrum to the downward moving rocket.

The flux values in the energy range 1.3 to 2.7 MeV have been calculated by subtracting the measured flux from 2.7 to 13 MeV, obtained in the coincidence channels

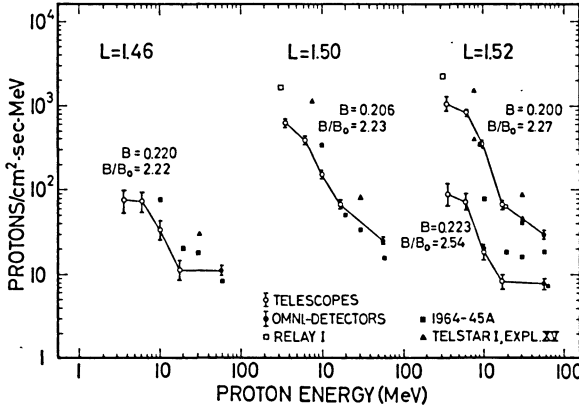


Figure 5: Differential omnidirectional protonflux  $L = 1.46$  to  $L = 1.52$ , vertical bars = statistical error.

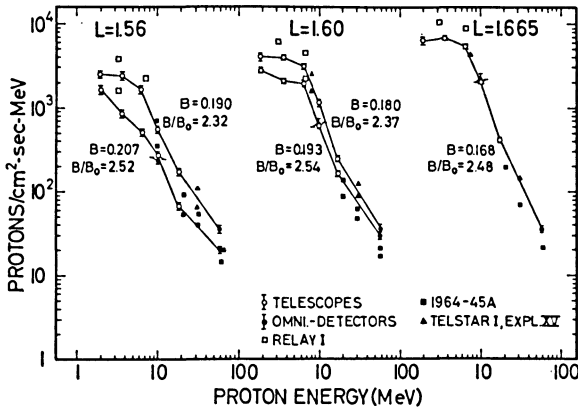


Figure 6: Differential omnidirectional flux  $L = 1.56$  to  $L = 1.665$ .

$IABC$ ,  $IABCD$ ,  $IIABC$  and with a correction in  $IIABCD$ , from the flux measured by the first detector in the energy range 1.3 to 13 MeV. Because of the greater uncertainty of the 13 MeV-boundary of channel A, this indicated value has a greater error than the one due to count rate statistics alone.

A possible electron contribution is given only by electrons  $> 600$  KeV, because those of lower energy are prevented to enter the detector stack by a magnetic field of about 1.7 KG in the aperture. As measurements showed the efficiency to detect electrons of  $E > 600$  KeV is smaller than  $5 \times 10^{-7}$  for the single detector channel IA taking into account the  $50 \mu$  thickness of the detector and the rather high threshold of about 18 times the average energy loss of minimum ionizing electrons. In the case of the channel IIA this corresponding factor is 7 and the detection efficiency is  $2 \times 10^{-5}$  for  $E > 600$  KeV, but increases with energy to values of about  $10^{-2}$  to  $10^{-1}$  for 1.0 or 2.5 MeV. Therefore, this channel is not used in the data.

The sensitivity to electrons of the coincidence channels is always smaller than  $10^{-7}$  and therefore the electron contribution to the counting rate is negligible. A pulse pile-up due to a high flux of electrons did not happen, since electrons above 300 KeV were monitored by the 1 mm-cube detector. The flux in the maximum was some  $10^5$  electrons/s  $\cdot$  cm<sup>2</sup>, with a corresponding number of incident electrons of less than  $10^4$ . A relative electron contribution therefore is less than  $10^{-4}$  of the actual counting rate.

Comparison of our omnidirectional proton measurements and those from the telescopes gives very good agreement where they overlap, around 10 MeV. This gives confidence in both sets of measurements and in the manner with which the directional data were converted to omnidirectional fluxes.

## Discussion

The RUBIS data are compared with the following results in Figs. 5 and 6:

1. Relay I in the energy range 2.5 to 3.8 MeV and 5.0 to 8.6 MeV [BROWN, DAVIDSON, MEDFORD 1964]. The unidirectional data have been transformed into omnidirectional fluxes.
2. Explorer XV in the energy range 4 to 13 MeV and Telstar I in the energy range 26 to 33 MeV [GABBE and BROWN, 1966].
3. 1964-45A in the energy ranges 6 to 20 MeV, 21 to 40 MeV, and 40 to 80 MeV [FREDEN, BLAKE and PAULIKAS, 1965].

These data are all taken near solar minimum, in the period from July 1962 to August 1964.

Comparison of our fluxes with those of the other experimenters are shown in Table 3 (see p. 36) with the absolute flux values and in Table 4 (see p. 37) and in Figure 7 with the ratio of our measured flux values (called  $\Phi$  Rubis) to the values of the other experimenters (called  $\Phi$  comp) as a function of the minimum mirror altitudes. The minimum mirror altitudes values were taken from BLANCHARD and HESS [1966]. In these regions where the flux gradient is steep, all the omnidirectional fluxes can be considered as mirroring fluxes and therefore the minimum mirror altitude will be a first approximate measure of the traversed atmospheric density.

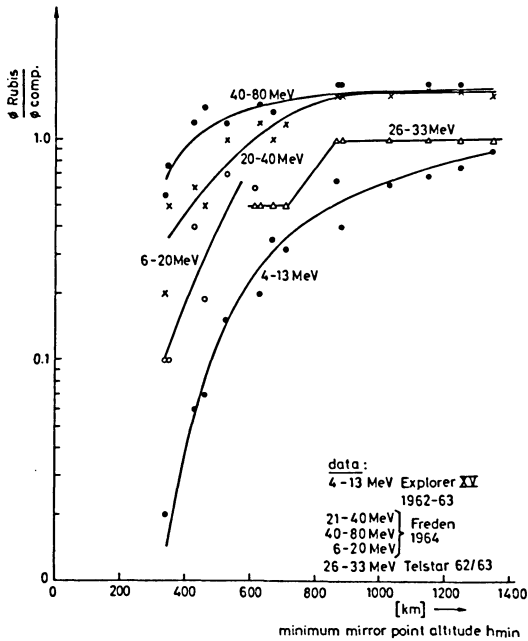


Figure 7: Comparison of RUBIS data with data of previous experiments taken near the South Atlantic Anomaly.

By comparing absolute flux measurements of different authors one has to consider error possibilities in

1. geometric factors,
2. contribution of electrons,
3. B-L-coordinate system.

Here it seems that the most important error possibility is the B-L-coordinate calculation taken for all these experiments (Jensen and Cain coefficients). Calculations of Heckman and Lindstrom [FREDEN et al., 1968], which compare the magnetic coefficients set of Jensen and Cain and the GSFC 1965 set, show for  $L = 1.4$ ,  $B = 0.24$  a difference of 0.005 Oersted and 0.003 L between the region of the Rubis shot (Longitude 0) and the south atlantic anomaly, where all other mentioned measurements are obtained. This difference leads to an about 50 km lower minimum altitude of all the Rubis data in the south atlantic anomaly. This difference in altitude due to a nonaccurate coordinate transformation has no effect on the flux comparisons, where the atmosphere losses are not the main ones or where the atmospheric density gradient is small enough. Therefore, for energies  $> 20$  MeV, the ratio of the measured fluxes is constant for  $h_{\text{min}} \geq 800$  km (Fig. 7). With decreasing altitude the scale height of

Table 3: Proton flux  $[N/(cm^2 \text{ sec MeV})]$  as measured with RUBIS experiments compared to other measurements.

$h_{min}$ L            B		40—80 MeV		21—40 MeV		26—33 MeV	6—20 MeV		4—13 MeV		5—8,6 MeV		2,5—3,8 MeV	
		Omnidir. RUBIS	Freden	Telesc. RUBIS	Freden	Telstar	Telesc. RUBIS	Freden	Telesc. RUBIS	Expl. XV	Telesc. RUBIS	Rel. I	Telesc. RUBIS	Rel. I
340	1,50	0,232	2,25	4,0	1,5±1,5	8,45		4,4±2	40	5±5	310			
350	1,44	0,226	3,84	5,00	5,2±3	10,5		4±4	46,5	5±5	730		18±16	
430	1,46	0,220	11,3	9,25	11±3	18,4		33±10	82	46±10	800		75±25	
460	1,52	0,223	7,85	5,50	8±1,5	15,8		18±8	103	32±6	455		87±25	
530	1,48	0,212	17,9	14,5	23±4	29,6		128±25	180	150	1000		230±60	
630	1,50	0,206	24,6	17,0	42±4	34,8	90	151±15	300	230	1110		610±60	1600
670	1,56	0,207	19,8	14,6	38±4	36,8	80	270		330	935		837	1770
710	1,52	0,200	29,2	18,7	45±5	38,5	90	341		440	1400		650	2150
870	1,60	0,193	30,2	17,0	75±7	47,5	70	602		950	1500		1500	3700
880	1,56	0,190	34,7	19,5	85±8	52,0	90	543		750	1900		1200	3700
1030	1,60	0,180	36,4	21,5	100±10	62,0	100	1144		1600	2560		2400	6150
1150	1,635	0,180	33,6	19,0	100±10	58,0	100	1700		1700	2560		2700	6800
1250	1,635	0,173	39,4	22,0	120±10	71,0	120	1593		2400	3220		3800	8700
1350	1,660	0,168	35,2	21,0	120±10	74,0	120	2016		2800	3900		4400	10400

Table 4: Ratios of the flux values of Table 3 (Rubis flux/flux measured by other authors). The errors are the statistical ones only.  
Where no error is indicated, the value is less than 10%.

$h_{min}$ [km]	L	B	40—80 MeV	21—40 MeV	26—33 MeV	6—20 MeV	4—13 MeV	5,0—8,6 MeV	2,5—3,8 MeV
			$\Phi_R/\Phi_{Fr}$	$\Phi_R/\Phi_{Fr}$	$\Phi_R/\Phi_{Teist}$	$\Phi_R/\Phi_{Fr}$	$\Phi_R/\Phi_{Expl.}$	$\Phi_R/\Phi_{Rel.}$	$\Phi_R/\Phi_{Rel.}$
340	1,50	0,232	0,56±15%	0,2±100%		0,1 ± 50%	0,02±100%		
350	1,44	0,226	0,77	0,5± 50%		0,1 ±100%	0,01±100%		
430	1,46	0,220	1,2	0,6± 20%		0,4 ± 30%	0,06± 25%		
460	1,52	0,223	1,4	0,5± 20%		0,18± 45%	0,07± 20%		
530	1,48	0,212	1,2	1,0± 15%		0,7 ± 20%	0,15± 15%		
630	1,50	0,206	1,45	1,2± 10%	0,5±10%	0,5 ± 10%	0,20± 10%		0,39±10%
670	1,56	0,207	1,35	1,0	0,5		0,35		0,47
710	1,52	0,200	1,6	1,2	0,5		0,32		0,46
870	1,60	0,193	1,8	1,6	1,0		0,65	0,65±10%	0,76
880	1,56	0,190	1,8	1,6	1,0		0,4	0,54	0,69
1030	1,60	0,180	1,7	1,6	1,0		0,62	0,54	0,67
1150	1,635	0,180	1,8	1,7	1,0		0,68	0,53	0,69
1250	1,635	0,173	1,8	1,7	1,0		0,75	0,58	0,69
1350	1,660	0,168	1,7	1,6	1,0		0,9	0,5	0,59

the atmospheric density decreases from a value of about 150 km at 800 km to about 50 km at 400 km altitude. In the same way the altitude difference of about 50 km steadily reduces with decreasing altitude the ratio of the fluxes measured inside and outside the anomaly to a third or a fifth of its value. Taking this into account, the proton flux of energies above 20 MeV agrees with the comparison data within less than a factor of two. This is in agreement with NAKANO and HECKMAN [1968] and FILZ [1967], who found a considerable time stability of proton flux at about 60 MeV down to 220 km altitude in the anomaly for the period 1962 to the beginning of 1966.

A quite different behaviour show the low energy data of the Rubis. In the energy region 4 to 13 MeV the flux measured by Rubis and by Explorer XV are nearly equal at 1350 km minimum altitude. Starting already at this altitude the fluxratio drops steadily with decreasing altitude to about 1/50 of its value. Unfortunately in the range  $2.5 < E < 8.6$  MeV there are only the comparison values of the Relay I satellite and they don't reach far into the atmosphere (Table 4). Neither the different altitude dependence nor the very low value of the fluxratio of the 4 to 13 MeV protons below 500 km minimum altitude can be explained by a systematic error due to the B, L computation as for the high energy protons. Since errors due to geometric factor for sure should be smaller than a factor of two and an electron contribution to the Explorer XV data at least in this region of space should be negligible [BROWN et al., 1964] we conclude that at least in the energy range 4 to 13 MeV the proton flux of 1966 has diminished significantly during the period 1962 to 1966. This applies only to minimum altitudes below about 500 km.

The reason for this change in intensity can either be a change in the source strength, whose mechanism for these low energies we don't know good enough, or a change in the atmospheric density or a combined effect. Since the lifetime of these low energetic protons is about a factor 5 smaller than the lifetime of the higher energetic ones of about 60 MeV, they should be more influenced by short time variations of the density. It might be that a solar cycle increase of the atmospheric density in 1966 has here its first measured effect on low energetic protons, whereas in August 1966 its effect is to be seen also in a reduction of the flux of 55 MeV protons [FILZ 1968]. But since it seems unlikely that the atmospheric density will change as much as the measured low energetic proton flux, one is lead to the assumption that the source strength will have changed too, perhaps in a certain way combined with the atmospheric density.

The shape and absolute flux values at energies above 10 MeV of this experiment are in good agreement with those of CRIFO and MOZER [1967] who measured the proton spectrum from 0.5 to 150 MeV over a similar but somewhat lower rocket trajectory at the same launching site in September 1965.

## Acknowledgements

We wish to thank Prof. R. LÜST for his support to our experiments as well as our colleagues E. KÜNNETH, P. LAEVERENZ, F. MELZNER, and F. STANEK for their help in performing and testing the instrument. We thank G. HAERENDEL for useful discussions.

We acknowledge the use of the Van de Graaff accelerators of the Siemens Research Laboratory, Erlangen, and of the Max-Planck-Institute for Nuclear Physics, Heidelberg.

## References

- ACHTERMANN, E.: Dissertation Max-Planck-Inst.-Bericht. MPI-PAE/Extraterr. 12/67
- BLANCHARD, R. C. and W. N. HESS: NASA TND 3086, 1966
- BROWN, W. L., L. N. DAVIDSON and L. V. MEDFORD: Bell Telephone Laboratory, Summit, New Jersey, 1964
- CRIFO, J. F. and F. S. MOZER: Phys. Rev. Letters, 19, 456, 1967
- FILZ, R. C.: J. Geophys. Res., 72, 959, 1967
- : Earth Particles and Fields, edited by B. McCormac, Reinhold Book Corporation, p. 15, 1968
- FREDEN, S. C., J. B. BLAKE and G. A. PAULIKAS: J. Geophys. Res. 70, 3133, 1965
- : Earth Particles and Fields, edited by B. McCormac, Reinhold Book Corporation, 1968
- GABBE, J. D. and W. L. BROWN: Radiation Trapped in the Earth Magnetic Field, edited by B. McCormac, p. 165, D. Reidel Publishing Company, 1966
- JENSEN, D. C. and J. C. CAIN: J. Geophys. Res. 67, 3568, 1962
- NAKANO, G. H. and H. H. HECKMAN: Phys. Rev. Lett. 20, 806, 1968

